

Detection and Characterization of Short Fatigue Cracks by Conduction Thermography [†]

Ester D'Accardi ^{1,*}, Davide Palumbo ¹ , Rosa De Finis ²  and Umberto Galietti ¹

¹ Department of Mechanics, Mathematics and Management, Politecnico di Bari, Via Edoardo Orabona, n.4, 70125 Bari, Italy; davide.palumbo@poliba.it (D.P.); umberto.galietti@poliba.it (U.G.)

² Innovation Engineering Department, Università del Salento, Campus Ecotekne Build. O-S.P. 6, Via Lecce Monteroni, 73100 Lecce, Italy; rosa.definis@unisalento.it

* Correspondence: ester.daccardi@poliba.it; Tel.: +39-348-737-7995

[†] Presented at the 17th International Workshop on Advanced Infrared Technology and Applications, Venice, Italy, 10–13 September 2023.

Abstract: Stimulated thermography is a very common non-destructive testing (NDT) technique used for a wide range of applications and materials. An external excitation source is required to stimulate the component and detect defects. Electric currents can be used in this sense adopting two different approaches: induction thermography and conduction thermography. In this work, a preliminary investigation to evaluate the influence of some test parameters during experiments of conduction thermography, for the detection of short fatigue cracks, induced in thin specimens of different materials, is presented. The capability of the technique and crack detectability have been analysed and compared with the Thermoelastic Stress Analysis (TSA) considered as a well-established technique capable of quantifying short fatigue cracks in metal materials.

Keywords: conduction thermography (CTT); fatigue cracks; Thermoelastic Stress Analysis (TSA)

1. Introduction

A component made of a conductive material can be inspected with the use of thermographic techniques in different ways and adopting several excitation sources. In this sense, induction and conduction thermography can be used [1–5]; with both approaches a current is induced within the inspected component, and depending on the current density and distribution, heating occurs in the component.

The use of induction thermography is very established and common for this kind of applications, with old and more recent publications [3–6], which have established limits and advantages in the application of the technique, also providing the POD curves (critical crack lengths) for different test conditions and geometric characteristics of the crack, as demonstrated in the work of Prof. Oswald-Tranta [6] with simulated and experimental data; instead, there are very few and old publications that proposed and discussed the conduction thermography technique (CTT) [1,2].

Basically, CTT is based on the transient temperature field under Joule effect heating generated by an electric current of a certain intensity (in DC or AC) [1]. The CTT allows to overcome the well-known problems related to the use of an induction coil (coil geometry and position with respect to the component). Moreover, another advantage is given by the possibility of using direct current (DC), that results homogeneously distributed if no defects are present [1] and allows to inspect deeper depths with respect to AC current.

In this work, an innovative and low-cost set-up is proposed to inspect several thin specimens of different materials by means of conduction thermography, adopting mainly a microbolometer sensor and a switching power supply up to 100 A. Pulsed (PT) and lock-in (LT) techniques have been applied, providing the capability of the technique and proposed approach to localize and quantify cracks. The obtained results were compared with those



Citation: D'Accardi, E.; Palumbo, D.; De Finis, R.; Galietti, U. Detection and Characterization of Short Fatigue Cracks by Conduction Thermography. *Eng. Proc.* **2023**, *51*, 23. <https://doi.org/10.3390/engproc2023051023>

Academic Editors: Gianluca Cadelano, Giovanni Ferrarini and Davide Moroni

Published: 1 November 2023



Copyright: © 2023 by the authors. Licensee MDPI, Basel, Switzerland. This article is an open access article distributed under the terms and conditions of the Creative Commons Attribution (CC BY) license (<https://creativecommons.org/licenses/by/4.0/>).

obtained by means of Thermoelastic Stress Analysis (TSA) [7–9] that can be considered a reference method.

2. Materials and Methods

The cracks have been generated by means of different cyclic tests with the MTS model 370 servo hydraulic fatigue machine with a 100 kN capacity (Figure 1a). Three different metal specimens have been analysed (see Table 1 for details), with a similar geometry (hole of 8 mm diameter, S1 $180 \times 38 \times 3 \text{ mm}^3$, S2 and S3 $200 \times 30 \times 1 \text{ mm}^3$).

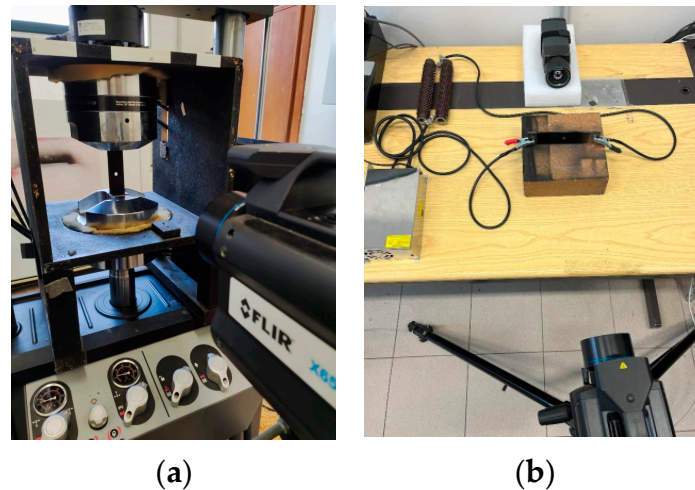


Figure 1. Adopted set-up for short fatigue crack generation and Thermoelastic Stress Analysis (TSA) (a) and the one used to perform conduction tests (b).

Table 1. Crack length estimation considering the results that come from the analysis of the different algorithms after a pulsed conduction test (100 A) with the cooled and microbolometer (uncooled) sensors and comparison with TSA.

Sp. ID	Material	Cooled PT Slope	Cooled PT R ²	Uncooled PT Slope	Uncooled PT R ²	TSA
S1	Titanium alloy	2.30 ± 0.15	2.10 ± 0.15	2.58 ± 0.14	2.43 ± 0.16	
S1 coat	Ti-6Al-4V	2.30 ± 0.23	2.58 ± 0.17	2.71 ± 0.17	2.57 ± 0.14	2.25 ± 0.15
S2	Ferromagnetic steel	1.40 ± 0.15	1.35 ± 0.15	1.40 ± 0.14	1.54 ± 0.14	
S2 coat		1.85 ± 0.17	1.55 ± 0.35	1.59 ± 0.14	1.59 ± 0.21	1.43 ± 0.15
S3	Austenitic steel	1.30 ± 0.15	1.55 ± 0.15	1.77 ± 0.21	1.35 ± 0.14	
S3 coat	AISI 304	1.60 ± 0.15	1.80 ± 0.15	1.82 ± 0.14	1.87 ± 0.16	1.43 ± 0.15

Thermoelastic data have been acquired by means of an infrared-cooled camera FLIR X6540sc with an indium-antimonium detector (FLIR Systems, Inc., Wilsonville, OR, USA, NETD < 25 mK, 640×512 pixels) and processed with the software IRTA 2. In particular, the specimens were tested applying a loading frequency equal to 13 Hz while sequences of ten seconds were acquired setting the frame rate to 200 Hz. For TSA tests, all the specimens have been painted with flat black coating for increasing emissivity value up to about 0.95.

Conduction tests have been carried out with the set-up shown in Figure 1b, considering two different infrared cameras placed on opposite sides of the specimen in order to monitor the crack length on both surfaces. In particular, the cooled camera X6540sc (lens 50 mm, MWIR, temperature range $12.7\text{--}86.4 \text{ }^\circ\text{C}$, integration time 0.57 ms, windowing 320×204 , spatial resolution 0.15 mm/pixel) has been used on one side and a microbolometer FLIR A655sc (FLIR Systems, Inc., Wilsonville, OR, USA, lens 25 mm, LWIR, temperature range $-40\text{--}150 \text{ }^\circ\text{C}$, NETD < 30 mK, windowing 640×240 pixels, spatial resolution 0.14 mm/pixel)

on the opposite side, trying to achieve the best resolution in both cases (however, no spacer ring has been added). A switching power supply has been adopted (12 V, 83.3 A), together with electrical resistors placed in series with the test specimens to avoid short circuits and change current levels (24, 37, 54, 74, 100 A). To set the pulse duration during pulsed tests (PT, frame rate cooled camera 500 Hz, microbolometer camera 100 Hz, pulse duration 2 s) and perform also lock-in tests (LT, frame rate 25 Hz, 3 cycles) with a square wave [10], a function generator has been used, together with a solid state relay to open and close the circuit. Furthermore, a clamp ammeter has been adopted to register for each test the effective current value. Different tests have been performed, changing the test parameters and repeating the tests 3 times, considering the specimens with and without black coating.

3. Procedure for Data Analysis and Results

To analyze data that come from conduction tests and to obtain from these some quantitative results for crack length estimation, common post-processing algorithms have been adopted, considering, for this preliminary work, the pulse thermal data and the heating phase. If a crack is present inside the inspected component, a localized temperature rise due to both the cross-section reduction and the concentration of the current distribution can be observed. Basically, it is possible to approximate the heating of the specimens with a straight line, and estimate the slope and square correlation coefficient R^2 , pixel by pixel.

The entire heating of almost 2 s can be evaluated, or only a part of it, to simulate different pulsed tests in the post-processing analysis [11,12]. Then, the sequences related to the contrast and the normalized contrast (CNR) [11] have been evaluated, considering a sound area near the crack (25×25 pixels²). An automatic routine that searches for the maximum value reached by each pixel for each investigated algorithm has then been used to identify the crack tip and quantify the crack length.

Finally, for TSA technique the position of the crack tip has been obtained applying Diaz's approach [7]. Diaz's method is a graphical approach based on the analysis of the characteristic phase signal trend along a line/profile passing through the crack tip [7].

4. Discussion

In Table 1 are reported some significant results obtained with CTT (only PT tests, for brevity) and TSA, as a comparison. In particular, for CTT, the mean and standard deviation value of 3 replications have been considered (when the standard deviation value is smaller than the test geometrical resolution this value is instead reported); for TSA a single measurement has been evaluated, and as standard deviation the measure of 1 pixel is considered. For brevity, these results are related to the pulsed conduction tests performed with a current value of 100 A and considering the specimens with and without black coating (for steel specimens the estimated emissivity value is around 0.2–0.3).

Some thermal maps are also shown in Figure 2 considering the results obtained for the titanium specimen (slope algorithm after CNR evaluation). In this case, and considering the slope algorithm, a time of about 0.1–0.2 s proved to be sufficient to obtain an indication around the crack tip. The obtained results also show the presence of a very small crack on the upper part of the hole (crack length \approx 0.5 mm). To be complete, for this material, some quantitative results ($\text{CNR} \geq 2$) have been obtained considering a current value of just 37 A for specimens with black coating, while it is necessary to reach 54 A to have a significant crack tip indication for uncoated specimens. The quantitative results reported in Table 1 for the crack length estimation by means of CTT show almost always a slight overestimation of the crack length, but in any case, in agreement with those obtained considering the TSA as reference technique.

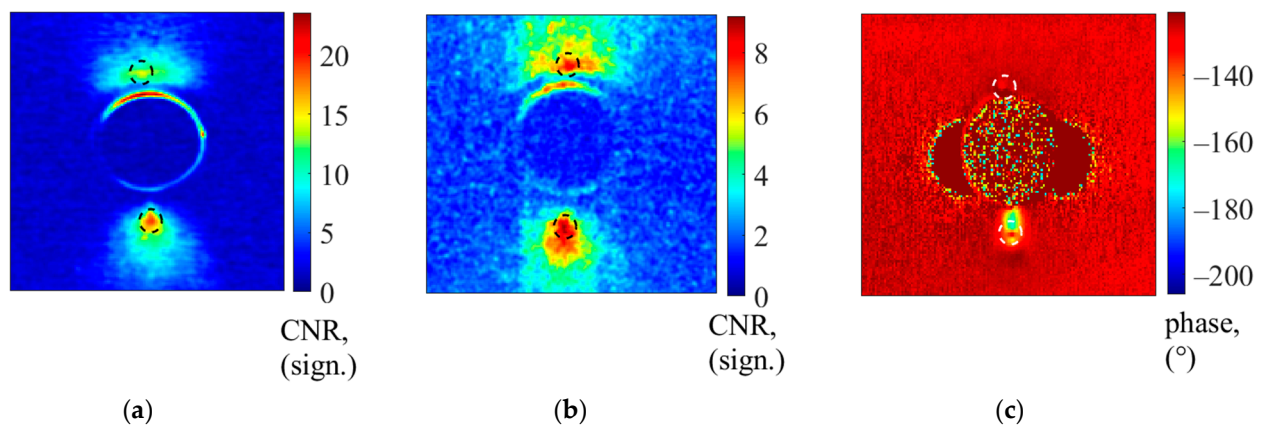


Figure 2. Comparison among the obtained results considering conduction thermography (100 A) and TSA as reference—titanium material: (a) slope results in terms of normalized maximum contrast with the cooled camera, (b) same algorithm and procedure with the acquisition of the microbolometer sensor and (c) phase map from TSA.

5. Conclusions

In this preliminary work, the capability of conduction thermography in fatigue crack detection has been demonstrated, investigating different specimens and materials.

Considering the adopted set-up, with low-cost devices, especially in terms of energy source, and the reached current levels, it has been possible to obtain quantitative results in agreement with those obtained with the TSA technique, but without the necessity to use a black coating to increase and uniform the emissivity.

However, the applicability of this technique depends on the electrical properties of the material and then to the current required to detect defects. Future developments will investigate the possibility of using the proposed technique and methodologies for crack monitoring, to demonstrate its possible application as a structural health monitoring (SHM) technique. The temperature variations due to the Joule's effect around notches and cracks appear very similar to the ones obtained with TSA. The possible relationship between the two techniques will be investigated in future works.

Author Contributions: Conceptualization, E.D. and U.G.; methodology, E.D., R.D.F. and D.P.; software, E.D., R.D.F. and D.P.; validation, E.D.; formal analysis, E.D. and R.D.F.; investigation, E.D., U.G. and D.P.; resources, U.G.; data curation, E.D., R.D.F. and D.P.; writing—original draft preparation, E.D.; writing—review and editing, E.D., R.D.F., D.P. and U.G.; visualization, E.D., R.D.F., D.P. and U.G.; supervision, U.G.; project administration, U.G.; funding acquisition, U.G. All authors have read and agreed to the published version of the manuscript.

Funding: Part of the work has been Financed by the European Union—NextGenerationEU (National Sustainable Mobility Center CN00000023, Italian Ministry of University and Research Decree n. 1033-17/06/2022, Spoke 11—Innovative Materials & Lightweighting). The opinions expressed are those of the authors only and should not be considered as representative of the European Union or the European Commission's official position. Neither the European Union nor the European Commission can be held responsible for them.

Data Availability Statement: The data presented in this study are available on request from the corresponding author.

Conflicts of Interest: The authors declare no conflict of interest.

References

1. Vrana, J.; Goldammer, M.; Bailey, K.; Rothenfusser, M.; Arnold, W. Induction and conduction thermography: Optimizing the electromagnetic excitation towards application. *AIP Conf. Proc.* **2009**, *1096*, 518–525.
2. Sakagami, T.; Ogura, K. New flaw inspection technique based on infrared thermal images under Joule effect heating. *JSME Int. J. Ser. A Mech. Mater. Eng.* **1994**, *37*, 380–388. [[CrossRef](#)]

3. Weekes, B.; Almond, D.P.; Cawley, P.; Barden, T. Eddy-current induced thermography—Probability of detection study of small fatigue cracks in steel, titanium and nickel-based superalloy. *Ndt E Int.* **2012**, *49*, 47–56. [[CrossRef](#)]
4. Oswald-Tranta, B. Induction thermography for surface crack detection and depth determination. *Appl. Sci.* **2018**, *8*, 257. [[CrossRef](#)]
5. Oswald-Tranta, B. Detection and characterisation of short fatigue cracks by inductive thermography. *Quant. InfraRed Thermogr. J.* **2022**, *19*, 239–260. [[CrossRef](#)]
6. Oswald-Tranta, B.; Hackl, A.; Lopez de Uralde Olavera, P.; Gorostegui-Colinas, E.; Rosell, A. Calculating probability of detection of short surface cracks using inductive thermography. *Quant. InfraRed Thermogr. J.* **2022**, *19*, 1–20. [[CrossRef](#)]
7. Diaz, F.A.; Patterson, E.A.; Tomlinson, R.A.; Yates, R.A. Measuring stress intensity factors during fatigue crack growth using thermoelasticity. *Fract. Eng. Mater. Struct.* **2004**, *27*, 571–583. [[CrossRef](#)]
8. De Finis, R.; Palumbo, D.; Di Carolo, F.; Ricotta, M.; Meneghetti, G.; Galietti, U. Crack tip position evaluation and Paris' law assessment of a propagating crack by means of temperature-based approaches. *Procedia Struct. Integr.* **2022**, *39*, 528–545. [[CrossRef](#)]
9. Pitarresi, G.; Patterson, E.A. A review of the general theory of thermoelastic stress analysis. *J. Strain Anal. Eng. Des.* **2003**, *38*, 405–417. [[CrossRef](#)]
10. D'Accardi, E.; Palumbo, D.; Galietti, U. A comparison among different ways to investigate composite materials with lock-in thermography: The multi-frequency approach. *Materials* **2021**, *14*, 2525. [[CrossRef](#)] [[PubMed](#)]
11. D'Accardi, E.; Palumbo, D.; Errico, V.; Fusco, A.; Angelastro, A.; Galietti, U. Analysing the Probability of Detection of Shallow Spherical Defects by Means of Pulsed Thermography. *J. Nondestruct. Eval.* **2023**, *42*, 27. [[CrossRef](#)]
12. Dell'Avvocato, G.; Gohlke, D.; Palumbo, D.; Krankenhagen, R.; Galietti, U. Quantitative evaluation of the welded area in Resistance Projection Welded (RPW) thin joints by pulsed laser thermography. In Proceedings of the Thermosense: Thermal Infrared Applications XLIV, Orlando, FL, USA, 6–12 June 2022; SPIE: Orlando, FL, USA, 2022; pp. 152–165.

Disclaimer/Publisher's Note: The statements, opinions and data contained in all publications are solely those of the individual author(s) and contributor(s) and not of MDPI and/or the editor(s). MDPI and/or the editor(s) disclaim responsibility for any injury to people or property resulting from any ideas, methods, instructions or products referred to in the content.